Determination of Crystal Growth Rate and Morphology of Barium Carbonate Crystals in a Semi-batch Crystallizer

Khorsand, Mohammad Reza
Faculty of Chemical Engineering, Amirkabir University, Tehran,, I.R. IRAN

Habibian, Mahmood*+; Rohani, Navid
Faculty of Chemical Engineering, Iran University of Science and Technology, Tehran, I.R. IRAN

Zarei, Ali Reza
Department of Chemistry, Malek Ashtar University of Technology, Tehran, I.R. IRAN

ABSTRACT: *A semi-batch crystallization system is used to determine growth kinetics and morphology of barium carbonate crystals, under a constant pH value and constant temperature in the various relative supersaturations. Results show that crystal growth rate satisfies a first-order kinetic expression at high relative supersaturation, while at relative supersaturation values lower than 3, the kinetic expression is second order. The crystal growth of barium carbonate follows the Burton, Cabera, and Frank mechanism by the kinetic expression* $G=\alpha\sigma^2 \tanh(\beta/\sigma)$*. The kinetic parameters obtained from low to high supersaturation ratio by using a numerical methods are* $\alpha=9.5\times10^{-7}$ ms^{-1} *and* $\beta=1.35\times10^{-2}$*. The investigations show that the pH values and relative supersaturation of solutions have an important role on the crystal morphology of barium carbonate and the forms of observed crystals are floc, candy-like, pillar-like, olivary and olivary with end dendrite with respect to operating condition.*

KEY WORDS: *Barium carbonate, Crystallization, Crystal growth, Crystal morphology, Precipitation.*

INTRODUCTION

Barium carbonate is an important raw material in industry for producing barium salts, pigments, optical glass, ceramic, electrical condensers and barium ferrite, super conductor and ceramic materials [1,2]. For manufacture of such raw materials, often a reactive crystallization process is used. Since the quality of

* *To whom correspondence should be addressed.*
+ E-mail: habana@iust.ac.ir
1021-9986/10/1/13 8/$/2.80

products and properties of powders, such as crystal size, crystal morphology and purity have an effect on the solid-liquid separation, an effective control on precipitation process is required.

Precipitation of barium carbonate in gas-liquid reactive crystallization by bubbling carbon dioxide in a solution of barium sulfide was studied by *Kubota et al.* [3] in two semi-batch reactors. They compared single-tube and double-tube gas injection nozzles. The result was that relatively large crystals with a pillar-like morphology were observed by using the double-tube, while small crystals with a thinner, needle-like morphology were found using the single tube. For growth kinetics mechanism they reported that the rate of $BaCO_3$ crystals was slightly changed with relative supersaturation.

In liquid-liquid reactive crystallization, precipitation and growth kinetics of barium carbonate was studied by several authors [4-6]. *Packter et al.* [4] found that the growth rate of $BaCO_3$ was proportional to an exponent of 1.4 in supersaturation. *Nore & Mersmann* [5] found that the growth mechanism at higher supersaturation, is diffusion controlled, while at lower supersaturation it becomes integration-controlled. *Chen et al.* [6] studied the morphology and growth kinetics of precipitation of $BaCO_3$ in a doble-jet semi-batch crystallization at constant pH values. They found that the morphology of $BaCO_3$ crystals depending on initial concentrations and pH values of solution and growth kinetics mechanism changes from diffusion step to surface-integration step, depending on the relative supersaturation.

Recently *Salvatori et al.* [7] considered the parameters such as pH value, Ba^{+2} ion concentration and temperature in precipitation process of barium carbonate. They found that crystal growth rates at high supersaturation satisfies a first-order kinetic expression while at supersaturation lower than 2, the kinetic expression is second order.

The aim of this work is to study the effect of operating parameters such as pH values, temperature, feed concentration on growth rate kinetics and particle morphology of barium carbonate crystals in a semi-batch crystallizer with a single feed addition of solution. To the best of our knowledge this is the first report on the precipitation of $BaCO_3$ crystals from reaction between barium sulfide solution and sodium carbonate solution.

THEORETICAL SECTION

Precipitation

Barium carbonate can be made from barium sulfide solution. BaS is the largest volume barium compound manufactured. It is readily soluble in water with hydrolysis, forming the hydroxide $Ba(OH)_2$ and hydrosulfide $Ba(SH)_2$. In the soda ash method sodium carbonate solution is treated with barium sulfide solution, producing barium carbonate and sodium sulfide. The Barium carbonate produced by precipitation is shown as following reaction [1]:

$$BaS+Na_2CO_3 \rightarrow Na_2S+BaCO_3 \quad (1)$$

The usual operating temperature is 60-70°C. In a centrifuge, barium carbonate is separated from sodium sulfide and the resulting slurry is filtered, washed and dried. The dried product was milled and packed finally [1].

$$S=\sqrt{\frac{a_{Ba^{2+}}a_{CO3^{2-}}}{K_{SP}}}=\gamma_{\pm}\sqrt{\frac{C_{Ba^{2+}}C_{CO3^{2-}}}{K_{SP}}} \quad (2)$$

Where a and C are ion activity and ion concentration, respectively, K_{SP} is the solubility product while $\gamma_{\pm}$ is the activity coefficient. The relative supersaturation of a $BaS\text{-}Na_2CO_3\text{-}H_2O$ solution is evaluated as follows:

$$\sigma = S-1 \quad (3)$$

In this method, aqueous systems containing Ba^{2+} and CO_3^{2-} ions also contain the ion pair, $BaCO_3^0$, the concentration of which is low and can be considered negligible in this study. Both activities $a_{Ba^{2+}}$ and $a_{CO_3^{2-}}$ are related to the activity coefficients and computed from the pH of the solution, barium ion concentration and carbonate ion concentration, using the activity coefficient equation proposed by *Davis* [9]:

$$\log\gamma_{\pm}=-0.509z_i^2\left(\frac{\sqrt{I}}{1+\sqrt{I}}-0.2I\right) \quad (4)$$

Eq.(4) gives a reasonable estimate of activity coefficients when the ionic strength, I; is smaller than 0.5 kmol/m^3. The ionic strength is defined as:

$$I=\frac{1}{2}\sum_i C_i Z_i^2 \quad (5)$$

where C_i is the concentration of i-component and z_i the charge number of i-component. At a given pH value and measured concentrations, the relative supersaturation can be determined when the activities of barium ion and carbonate ion are obtained.

The relative supersaturation is based on the assumption that two reactants are immediately and completely macro mixed and micro mixed with bulk liquid already in crystallizer, because the local supersaturation distribution is not known. Therefore, the measured supersaturation ratio is a mean value. Different solubility products for barium carbonate have been reported in the literatures. *Nore & Mersmann* [5] used the value of 1.23×10^{-8} mol^2l^{-2}, while *Chen* [6] accepted the value given by *Kortly & Sucha* [10], which is 5.0×10^{-9} mol^2l^{-2} and *Salvatori* [7] accepted the value given by *Lide* [11] that is 2.58×10^{-9} mol^2l^{-2}. Many other values can be obtained from data banks and literatures, but in our study, we accept the value used by *Chen* [6] that is 5.0×10^{-9} mol^2l^{-2}.

EXPERIMENTAL SECTION

Materials and Methods

A semi-batch crystallization system used for the liquid-liquid reactive crystallization study of barium carbonate is shown in Fig. 1. The system consists of conductimeter, pH controller, a one liter crystallizer, an injection pump, a thermal bath and a variable speed agitator.

At the beginning, 500 cc of barium carbonate suspended solution was dispensed into the crystallizer. The desired pH value was adjusted by adding 0.1 M of NaOH or 0.1 M HCl solutions, subsequently the pH is kept constant during the precipitation process. The operation was performed in a pH range of 10–11.5 and the speed of rotation was set at 350 rpm for complete operation time of 20 minutes. At the same time, sodium carbonate (Na_2CO_3) solution with a known concentration was discharged into the crystallizer. Then, barium sulfide (BaS) solution with a desired feed rate (ml/min) was allowed to enter the reactor through the injection pump. In order to minimize the effect of micro mixing on the crystal size distribution at the initial stages, the feed concentration of barium sulfide was the same as that of the concentration of the sodium carbonate already in the crystallizer. The precipitation experiments were conducted in the temperature range of 58-70 °C. The temperature was controlled and kept constant by thermal bath during the process.The barium ion concentration in the solution determined by conductimeter which gives the concentration for different time. Samples of solution were withdrawn by syringe every 4 minutes and filtered with a 0.1 μm filter, through vacuum process to remove solid crystals. The mean particle size of barium carbonate crystals and its morphology were determined by scanning electron microscopy SEM (XL30-Phillpis-Netherlands). The operating conditions maintained in this study are listed in Table 1.

Table 1:Operating conditions.

Concentration of Na_2CO_3 at initial stage (mM)	4-7
Feed rate of BaS (ml/min)	1-2.5
Feed concentration (mM)	4-7
pH range	10-11.5
Operating temperature (^{0}C)	58-70
Concentration of NaOH(M)	0.1
Concentration of HCl(M)	0.1
Speed of stirring (rpm)	350
Operating time(min)	20

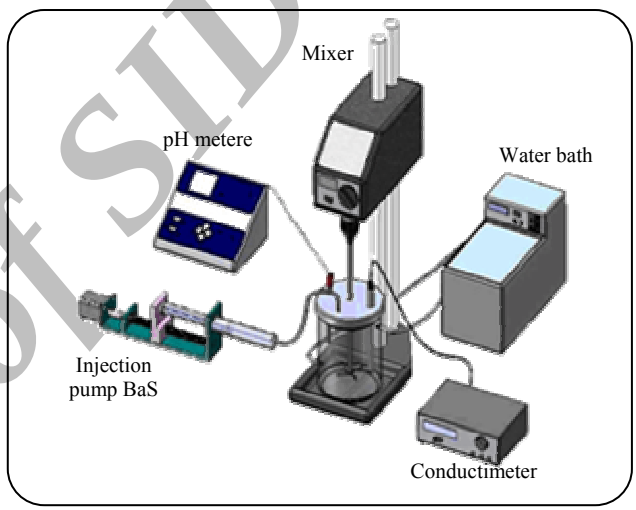

Fig. 1: The crystallization system 1.

RESULTS AND DISCUSSION

Determination of crystal growth kinetics

In a precipitation process, the crystal growth rate is a crucial parameter, since it determines the final specific properties of crystals such as morphology and the mean size of particles. In order to obtain these kinetic parameters, in a semi-batch mode, the experiments allow

a study within a relatively short time, but the exploitation of experimental results is complicated by the time variation of supersaturation and mean particle size. It is proved that this mode can be successfully used for the systems of very rapid crystal growth kinetics for barium carbonate as a precipitation substance.

The growth rate of barium carbonate crystals can be evaluated by the following definition at any stage:

$$G = \left.\frac{d\bar{L}}{dt}\right|_t \qquad (6)$$

Where $\bar{L}$ is the mean particle size obtained from the measured data (Fig.2). The mean particle size varies with time and can be expressed as a polynomial function. For example, the function obtained from run no. 14 is expressed as follows:

$$\bar{L} = 1\times10^{-5} + 11\times10^{-5}\,t + 1\times10^{-5}\,t^2 + 1\times10^{-5}\,t^3 + 1\times10^{-5}\,t^4 \qquad (7)$$

By substituting Eq. (7) in to Eq. (6), the linear growth rate in any time stage can be obtained.

In the Eq.(6), the crystal growth rate, G(t) is replaced by its expression as a function of relative supersaturation. First we assume that the crystal growth is integration controlled with minimum diffusional limitation (this assumption will be checked next). Several expressions can be used to link growth rate to relative supersaturation. The most classical is the power law relationship as follows:

$$\frac{d\bar{L}}{dt} = G(t) = K\sigma^n \qquad (8)$$

Where K and n are the kinetic constants and σ is the relative supersaturation as defined in Eqs. (2) and (3).

Second we assume the migration to the surface as the limiting step*; Burton, Cabera & Frank* [12] have proposed a growth rate expression of the following form:

$$G(t) = \alpha\sigma^2 \tanh\left(\frac{\beta}{\sigma}\right) \qquad (9)$$

Where α and β are kinetic parameters and σ is the relative supersaturation (as defined in Eqs. (2) and (3)).

By substituting Eq. (9) into Eq. (6); the differential equation gets the following form:

$$\frac{d\bar{L}}{dt} = \alpha\sigma^2 \tanh\left(\frac{\beta}{\sigma}\right) \qquad (10)$$

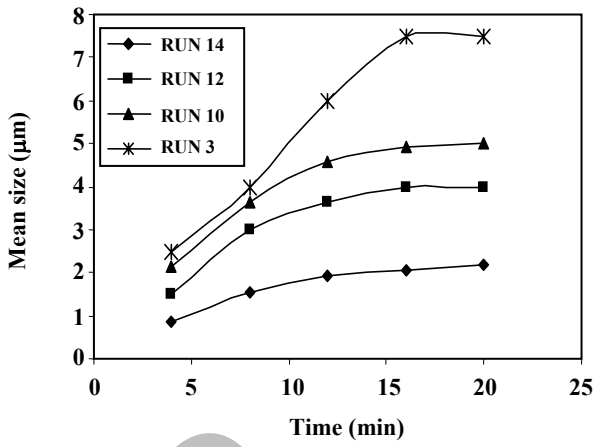

Fig. 2: Mean particle size versus time.

Where in both Eqs. (8) and (10) the relative supersaturation is a function of operating time.

$$\sigma = \sigma(t) \qquad (11)$$

To obtain this function, we express relative supersaturation; Eq. (2) and Eq. (3), with a conversion mode:

$$\sigma = C_0\gamma_{\pm}\sqrt{\frac{(1-X)(M-X)}{K_{SP}}} - 1 \qquad (12)$$

While conversion X and initial stoichiometric ratio M are expressed by the following formula:

$$X = \frac{C_0 - C}{C_0} \quad \text{and} \quad M = \frac{\left[CO_3^{2-}\right]_0}{\left[Ba^{2+}\right]_0} \qquad (13)$$

The variation of conversion against time can be followed by conductimetry. The *Salvatori*'s method [7] is used for obtaining expression between conversion and conductivity, as follow:

$$x_0 - x = \frac{2C_0X}{1000}\left(\lambda_{Ba^{2+}} + \lambda_{CO_3^{2-}}\right) \qquad (14)$$

Where x is conductivity (Scm^{-1}) and λ is equivalent ionic conductivity (cm^2Smol^{-1}).

The relative supersaturetion, and the variation of mean particle size $\bar{L}$ at any time is calculated and substitute in to the Eq. (8) and Eq. (10). The kinetic parameters, k and n of Power law model and α and β of Burton model, determined by using numerical integration.

Effect of relative supersaturation

Fig.3 shows the effect of feed concentration on the elapsed time of relative supersaturation for three typical runs, Nos. 10, 11, and 12 at a pH of 11. The results show that the relative supersaturation at higher feed concentrations was higher than that at lower feed concentrations, since the concentration of barium ions was higher at higher feed concentrations.

However, all of the relative supersaturations come to a lower value around an elapsed time of 20 minutes, and remains almost constant. Furthermore, all of the relative supersaturations come together gradually, since the cumulative carbonate increases to a higher value for the lower feed concentrations. In any case, the effects of feed concentration on elapsed time of relative supersaturation are obviously significant at the initial stage and the effects are reduced after 20 min of operation.

For power law model; in low relative supersaturation values ($\sigma<3$) the order of the crystal growth rate is close to 2 with a kinetic constant k of 1.8×10^{-9} $m^4mol^{-1}s^{-1}$, that is the crystal growth is mostly controlled by the surface integration and follows :

$$G(t)=1.8\times10^{-9}\ \sigma^{1.92} \qquad (15)$$

Fig. 4 illustrates the determination of growth rate in low relative supersaturation values using Eq. (15).

For power law model, in high relative supersaturation values, all experiments have lead to kinetic order close to 1 and the calculated value for k is 3.4×10^{-9} $m^4mol^{-1}s^{-1}$. Therefore in this case the crystal growth is mostly controlled by the diffusion and follows :

$$G(t)=3.4\times10^{-9}\ \sigma^{1.11} \qquad (16)$$

Fig. 5 illustrates the determination of growth rate in high relative supersaturation values using Eq.(16).

A plot of log G versus log σ is shown in Fig. 6. The slopes for low supersaturation are close to 2, and for high supersaturation is close to 1, which is similar to the results reported by *Nore & Mersmann* [5].

As the order of crystal growth rate follows Eq. (15) and Eq. (16) for power law model, therefore the crystal growth mechanism in this case can be suppose to follows *Burton*, *Cabrera & Frank* model [12] expressed by Eq.(9). The kinetics parameters $\alpha=9.5\times10^{-7}$ ms^{-1} and $\beta=1.35\times10^{-2}$ are obtained by numerical integration and least-squares techniques of Eq. (10). Therefore the result for growth rate is as follows:

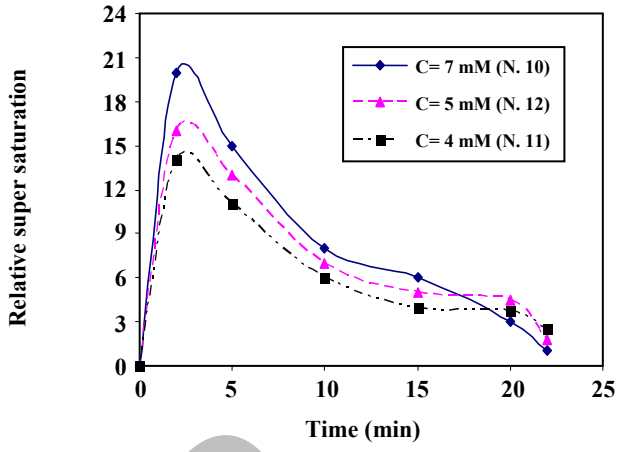

Fig. 3: Elapsed time of relative supersaturation at different feed concentration, pH=11.

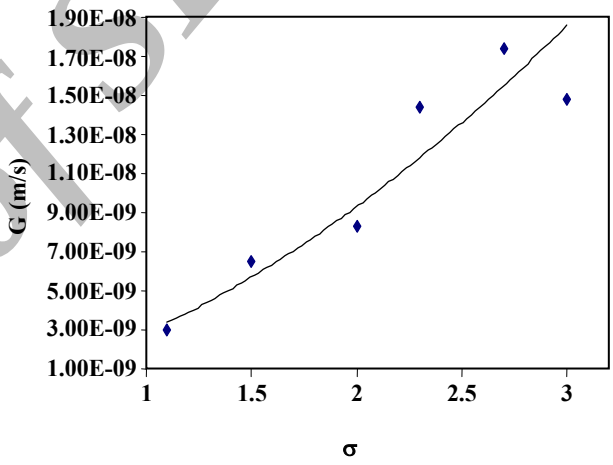

Fig. 4: Growth rate in low supersaturation.

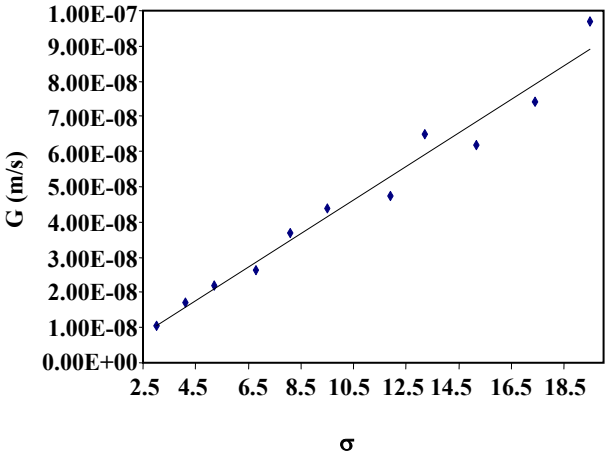

Fig. 5: Growth rate against high supersaturation.

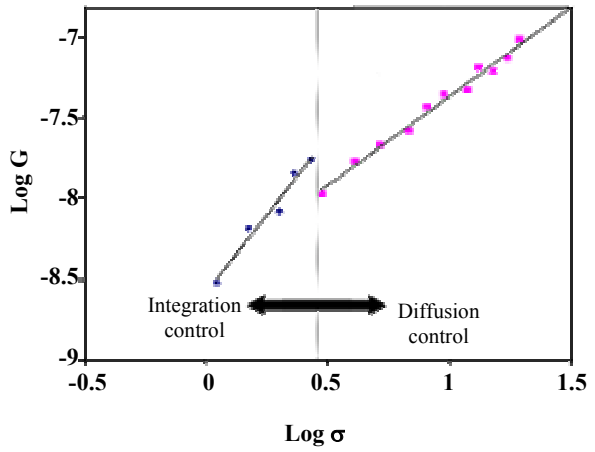

Fig. 6: Growth mechanisms versus relative supersaturation.

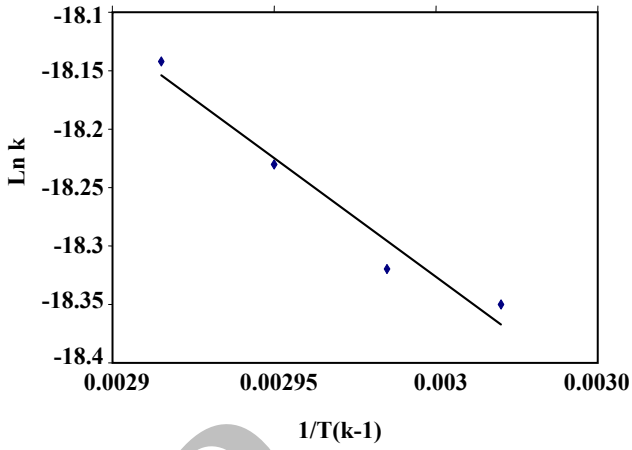

Fg. 7: Influence of temperature on crystal growth rate constant k.

$$G(t)=9.5\times10^{-7}\,\sigma^{2}\tanh\left(\frac{1.35\times10^{-2}}{\sigma}\right) \qquad (17)$$

Effect of temperature

Temperature affects crystal growth rate as it can be sufficient to produce diffusion controlled growth at high temperature, compared to integration step controlled at low temperature. The influence of temperature is studied by realizing experiments in the range of 58-70 °C. The results show (Fig. 7) that the kinetic constant k follows an expression according to Arrhenius law and follows by Eq. (18). This result is similar to that reported by *Salvatori* [7].

$$k=9.3\times10^{-6}\exp\left(-\frac{2040}{T}\right) \qquad (18)$$

The expression presented above are obtained in high temperature and assuming that the surface integration has more influence on crystal growth than mass transfer. To verify this hypothesis, the crystal growth rate constant and mass transfer coefficient, calculated by expressions proposed by *Nore & Mersman* [5], are used to determine the effectiveness factor according to *Garside's* method [12]. In most cases, we have obtained an effectiveness factor close to 1, proving that the crystal growth takes place in the surface integration limitation more than diffusion controlled regime.

Effect of pH

The experiments are carried out at different pH value varied by adding a quantity of sodium hydroxide. At pH value higher than 10, bicarbonate ion is shifted to carbonate ion which plays the major role in the solution [12]. Therefore, in the range of pH from 10 to 11.5, the variation of carbonate ion in solution is less affected by pH. Thereby the kinetics constant k of growth rate is less influenced by variation of pH, which is similar to results, reported by *Salvatori et al.* [7].

Morphology of crystals

In considering the morphology of crystals it was found that the solution concentration and pH of solution had a significant effect on the morphology of barium carbonate crystals. Fig. 8. shows the photographs of precipitated crystals which are taken by SEM.

The results indicate that there are five major shapes as, floc, candy, olivary with end dendrite, pillar-like and olivary. *Kubota et al.* [3] and *Chen et al.* [6] also have reported similar results.

The pillar-like crystals are the most morphology obtained at high concentration and high pH values. At high to moderate concentration, the floc precipitation is the major products obtained in the pH range of 10-11.5. At moderate to low concentration, the olivary crystals and candy crystals become the major products in the pH range of 10-10.5. The olivary crystals with end dendrite are observed when the pH value is around 11 and higher. Finally, the results also show that with similar relative supersaturation, the corresponding growth rate, decreases in the order of floc>candy> olivary>olivary-with end dendrite> pillar-like, which is similar to the results obtained by *Chen et al.* [6].

CONCLUSIONS

A semi-batch crystallization system was successfully designed to study the growth kinetics and morphology of barium carbonate crystals. The growth kinetics changes in turn from diffusion step at high relative supersaturation to surface integration step, at low relative supersaturation. The temperature has a pronounced effect on crystal growth rates. It is mostly surface integration-controlled regime at high temperature and the relationship on growth kinetics follows an expression according to Arrhenius law. It was also shown that the morphology of barium carbonate crystals varied with respect to initial concentration and pH value of the solution. The major products at high concentration and pH values are floc and pillar-like crystals, while at low pH and concentration, olivary-like crystals form. Finally, the growth kinetics and morphology of barium carbonate can be controlled by pH, concentration and temperature of the solution when the operation is adjusted to desirable operating conditions.

Nomenclature

S	Supersaturation ratio
a_{Ba}^{2+}	Activity for barium ion (mol/lit)
a_{CO3}^{2-}	Activity for carbonate ion (mol/lit)
C	Ion concentration (mol/lit)
$\gamma_{\pm}$	Activity coefficient
σ	Relative supersaturation
$BaCO_3^0$	Iion pair
I	Ionic strength
Ci	Concentration of i-component (mol/lit)
zi	Charge number of i-component
G	Crystal growth rate (m/s)
$\overline{L}$	Mean particle size (m)
t	Time (min)
k	Kinetic constant in power law model (m/s)
n	Power exponent in power law model
α	Pre-hyperbolic growth rate constant (m/s)
β	Hyperbolic growth rate constant
X	Conversion
M	Initial stoichiometric ratio
x	Conductivity (Scm^{-1})
λ	Equivalent ionic conductivity (cm^2Smol^{-1})
T	Temperature (^oC)
K_{sp}	Solubility products ($mol^2\ l^{-2}$)

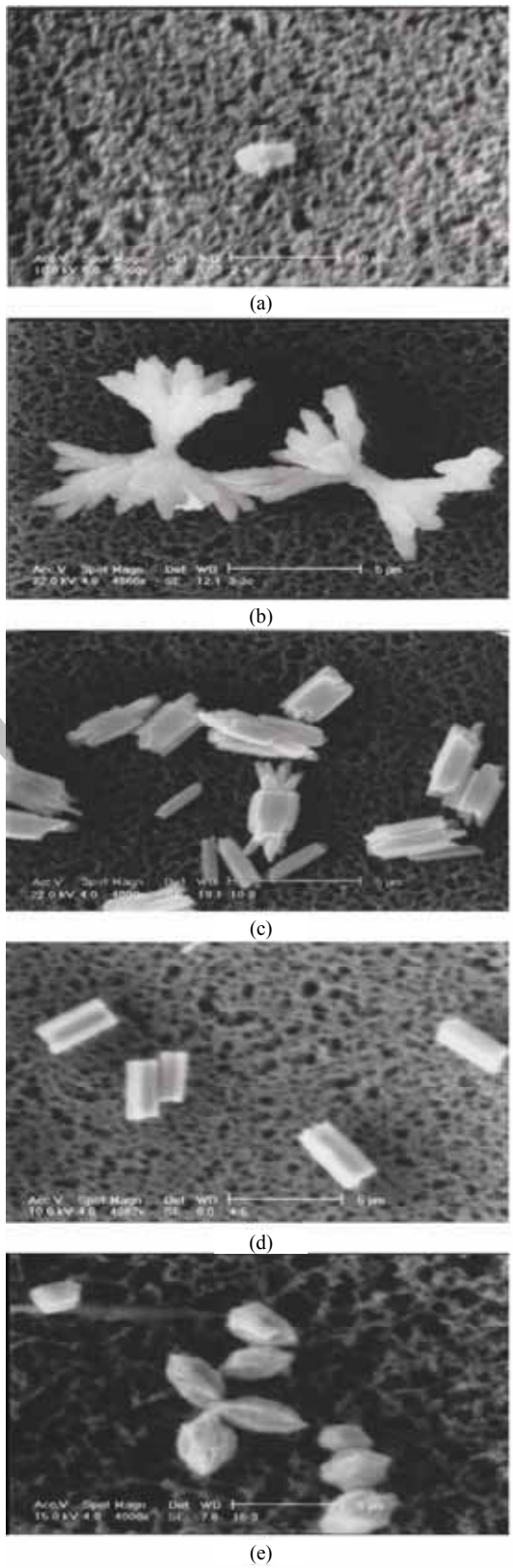

(a) (b) (c) (d) (e)

Fig. 8: Mophology of BaCO3 crystals: (a) Floc (b) Candy (C) Olivary with end denderite (d) Pillar-like (e) Olivary.

Table 2: Design of experiment.

Run	pH	Temp	concentration	Feed rate
1	10	58	4	1
2	10	62	5	1.5
3	10	66	6	2
4	10	70	7	2.5
5	10.5	58	5	2
6	10.5	62	4	2.5
7	10.5	66	7	1
8	10.5	70	6	1.5
9	11	58	6	2.5
10	11	62	7	2
11	11	66	4	1.5
12	11	70	5	1
13	11.5	58	7	1.5
14	11.5	62	6	1
15	11.5	66	5	2.5
16	11.5	70	4	2

Appendix

The Details of experimental conditions from run number 1 to 16 are as follow Table [2].

Received : July 20, 2008 ; Accepted : Feb. 3, 2009

REFERENCES

[1] Maketta J.J., "Encyclopedia of Chemical Processing and Design ", Marcell Dekker, Inc New York, p.51 (1977).

[2] Allen B.F., Faulk N.M., Lin S.C., Semiat R., Luss D., Richardson J.T., "A.I.Ch.E. Symp. Ser.", **88**, p. 76 (1994).

[3] Kubota N., Sekimoto T., Shimizu K., Precipitation of $BaCO_3$ in a Semi-batch Reactor with Double-tube Gas Injection Nozzle, *J. Crystal Growth*, **102**, p. 434 (1990).

[4] Packter A.J., The Precipitation of Sparingly Soluble Alkaline-Earth Metal and Lead Salts: Nucleation and Growth Orders During the Induction Period, *J. Chem. Soc.*, **Series A**, p. 859 (1968).

[5] Nore Ph., Mersmann A., Batch Precipitation of Barium Carbonate, *Chem. Eng. Sci.*, **48**, p. 3083 (1993).

[6] Chen P.C., Nucleation and Morphology of Barium Carbonate Crystals in a Semi-batch Crystallizer, *J. Crystal Growth*, **226**, p. 458 (2001).

[7] Salvatori F., Determination of Nucleation and Crystal Growth Kinetics of Barium Carbonate, *Powder Technology*, **128**, p. 114 (2002).

[8] Nancollas G.H., "Interactions in Electrolyte Solutions", Elsevier, Amsterdam, , p. 25 (1966).

[9] Butler J.N., "Ionic equilibrium|", Addision-Wesley publishing, Co., Inc., MA (1964).

[10] Lide D.R., (Ed.), "Handbook of Chemistry and Physics", 80th ed., CRC Press, pp. 8-111 (1999-2000).

[11] Burton W.K., Cabrera N., Franck F.C., The Growth of Crystals and the Equilibrium Structure of their Surface, *Philos. Trans. R. Soc. Lond.*, **243**, p. 299 (1951).

[12] Garside, J., Effectiveness Factors in Crystal Growth, *Chem.Eng. Sci.*, **26**, p. 1425 (1971).